



## Experimental study of the microbial fuel cell internal resistance

Zhang Pei-Yuan, Liu Zhong-Liang\*

The Education Ministry Key Laboratory of Enhanced Heat Transfer and Energy Conservation, Beijing University of Technology, Beijing 100124, China

### ARTICLE INFO

#### Article history:

Received 13 May 2010

Received in revised form 18 June 2010

Accepted 18 June 2010

Available online 25 June 2010

#### Keywords:

Microbial fuel cell

Internal resistance

Current

Limiting current

Concentration loss

### ABSTRACT

The internal resistance, including activation loss internal resistance (AIR), ohmic loss internal resistance (OIR) and concentration loss internal resistance (CIR), is an important parameter that determines the performance of microbial fuel cells (MFCs). The experimental investigations were completed to estimate the contributions of these three components to the internal resistance. The internal resistance is found to vary with electric current, although it is almost a constant for the current is within a certain region. The largest component of the internal resistance is CIR except for small currents. The AIR decreases quickly for small current and reduces its decreasing rate as the current increases and approaches to a constant. The OIR is constant over the whole current range. The experiments also disclose that increasing the limiting current and reducing the concentration loss are both important for improving the MFC performance.

© 2010 Elsevier B.V. All rights reserved.

### 1. Introduction

At present, reducing environmental pollution and exploring new energy sources are the two important measures to achieve sustainable development and circulation economy. Microbial fuel cell (MFC) is one of the new technologies that do the both at the same time. The MFCs use micro-organisms as biological catalyst to directly convert organic biomasses, which may be considered as a type of pollution, into electrical energy. A variety of wastewater can be used as raw materials. MFC has many advantages over the traditional technologies, such as the diversification of fuel sources, non-pollution, high energy efficiency, mild operating conditions, strong biocompatibility, and so on. Due to all these advantages and its great application potential in various areas such as microbial sensors, bioremediation, sewage treatment, this technology has received more and more attention from both governments and scientists.

A MFC usually consists of an anode chamber and a cathode chamber physically separated by a proton exchange membrane (PEM). Micro-organisms in the anode chamber form a mini-ecosystem harvesting energy and generating protons and electrons by oxidizing substrates in anaerobic environment. When operating, protons travel through the PEM, and electrons travel through the external circuit to the cathode chamber, where they are consumed to reduce oxygen to water.

Low power output is the biggest disadvantage of the MFC technology at present (three orders of magnitude smaller compared with a fuel cell). The internal resistance of a MFC is closely related to the power output. The particular internal resistance that results in the largest power output is used as an important parameter to evaluate MFC performances in most literatures. Several different methods for evaluating the MFC internal resistance were summarized in [1]. Cao and Liang made a membrane electrode assembly (MEA) typed MFC, and found that the internal resistance was about 10–30  $\Omega$  under the steady state operation conditions [2]. Liang and Fan used carbon nanotube, flexible graphite and activated carbon as anode material, and found that the internal resistances were 263  $\Omega$ , 301  $\Omega$  and 381  $\Omega$ , respectively [3]. Min and Angelidaki constructed a submersible MFC, and found that the internal resistance was  $35 \pm 2 \Omega$  [4]. Wen and Liu fabricated an air–cathode MFC, and found that the internal resistance was 33.8  $\Omega$  [5]. He [6] used the internal resistance as a parameter to define the UMFC performance, and analyzed several factors affecting the internal resistance. Manohar and Mansfeld divided the internal resistance into three parts, namely the cathode polarization resistance, the anode polarization resistance and the ohmic resistance. The idea is actually from electrochemistry and is used to present the influences of the electrode materials and electrode configuration on MFC performances [7]. The composition of the MFC internal resistance was obtained based on electrical knowledge and a one-dimensional model of fuel cells, which ignored the effects of electrodes on the MFC performance. Therefore, it is important to separate or split the MFC internal resistance according to microbial fuel cell itself to get an accurate and insight understanding of the MFC process. Hence an experimental study is carried out in this paper to deter-

\* Corresponding author. Tel.: +86 10 67391917; fax: +86 10 67391917.  
E-mail address: [liuzhl@bjut.edu.cn](mailto:liuzhl@bjut.edu.cn) (Z.-L. Liu).

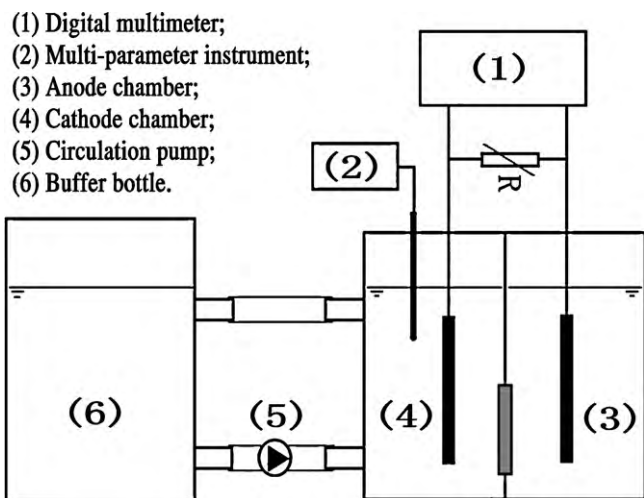


Fig. 1. Schematic diagram of the MFC.

mine the contributions of the internal resistance components of MFC and the influences of various factors on the internal resistance are discussed, trying to provide a theoretical basis for reducing MFC internal resistances and optimizing MFC configurations.

## 2. Materials and methods

### 2.1. MFC construction

The MFC used in this paper is composed of two 1300 ml plexiglass chambers that act as anode and cathode. Each chamber has three ports on the top that are used for gas-outputting, sampling and electrode probing, respectively (Fig. 1). These ports are all sealed with butyl stoppers and fixed with screw caps. Two chambers were separated by a PEM (5.0 cm × 5.0 cm, Nafion-117, Dupont) and assembled using stainless steel studding, washers and nuts. Each chamber contained two pieces of graphite felt with an effective surface area of 100 cm<sup>2</sup> each. The electrodes are connected with copper wire to provide the connections for the external circuit. A resistance box (ZX36, China; range: 0–9999 Ω, accuracy: 1 Ω) is used as the external circuit load. The voltage is measured by a digital multimeter (UT70D, China; range: 0–800 mV, accuracy: 0.1 mV) and recorded by a personal computer.

### 2.2. Anode inoculation and operation

Activated sludge from Beijing Gaobeidian wastewater treatment plant is used as inoculum, and was domesticated and cultured in anode solution for 3 weeks. Sterilized deionized water is used as solvent. Synthetic wastewater [8] containing sodium acetate as the carbon source is used as the anode solution in this study unless specified. It is prepared by adding 1000 mg sodium acetate, 10,020 mg NaCl, 681 mg KH<sub>2</sub>PO<sub>4</sub>, 117 mg NaOH and 20 ml solution of rare metal elements and vitamin per unit liter deionized water. Its COD concentration is 850 mg l<sup>-1</sup> approximately. Cathode solution is prepared by adding 10,020 mg NaCl, 681 mg KH<sub>2</sub>PO<sub>4</sub> and 117 mg NaOH per unit liter deionized water, and potassium ferricyanide (K<sub>3</sub>Fe(CN)<sub>6</sub>, 1000 mg l<sup>-1</sup>) is used as the electron acceptor. The chambers are flushed with nitrogen gas for 2 min to remove dissolved oxygen so as to maintain anoxic conditions. The MFC was operated in fed-batch mode at a fixed load (1000 Ω, unless stated otherwise). The MFC was operated at room temperature varying between 17 °C and 23 °C. The relative humidity was 15–45%. The cathode solution is circulated with a buffer bottle of 2000 ml at a

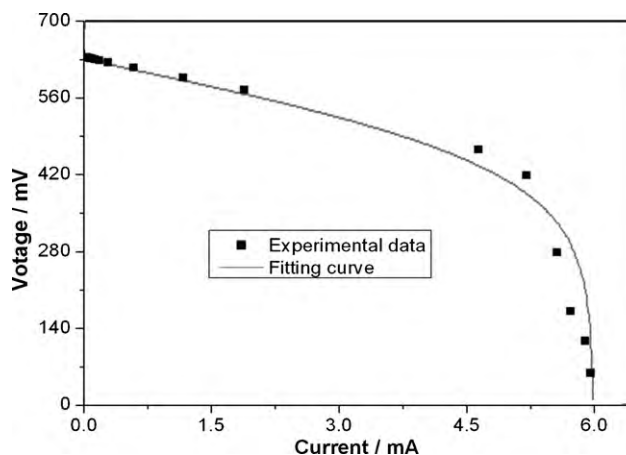


Fig. 2. Steady state voltage generated as a function of the current.

mass flow of 350 l h<sup>-1</sup> by a circulation pump to ensure adequate supply of the electron acceptor.

### 2.3. Data acquisition and calculation

Voltage was measured using a digital multimeter (UT70D, China; range: 0–800 mV, accuracy: 0.1 mV). Polarization curves were obtained by varying the external resistance over a range from 10 Ω to 9999 Ω when the voltage was kept constant. Ambient temperature and relative humidity were measured using a temperature and humidity meter (Rotronic K15, Sweden; temperature—range: 0–100 °C, accuracy: 0.1 °C; relative humidity—range: 0–100%, accuracy: 0.1%). Ionic conductivity was measured using a multi-parameter instrument (Multi 340i, Germany; range: 0–199.9 S m<sup>-1</sup>, accuracy: 0.1 S m<sup>-1</sup>).

Electric current, power and the internal resistance are calculated from Eqs. (2.1), (2.2) and (2.3), respectively.

$$I = \frac{V}{R_o} \quad (2.1)$$

$$P = IV \quad (2.2)$$

$$R_i = \left( \frac{E_t}{V} - 1 \right) R_o \quad (2.3)$$

where  $V$  is the electric voltage, V;  $R_o$  and  $R_i$  are external and internal resistances, Ω;  $I$  the electric current, A; and  $E_t$  is the electromotive force, V.

## 3. Results and analysis

### 3.1. Analysis of internal resistance

The MFC voltage losses mainly include the activation or reaction kinetics, the ohmic polarization and the concentration or mass transport losses. The real voltage output for a MFC can thus be calculated by subtracting the voltage drops due to the various losses from its electromotive force and then [9]:

$$V = E_t - \eta_{act} - \eta_{ohmic} - \eta_{conc} \quad (3.1)$$

where,  $\eta_{act}$ ,  $\eta_{ohmic}$  and  $\eta_{conc}$  are voltage losses due to reaction kinetics, ohmic polarization and mass transport, respectively.

Polarization curves are useful for determining the dependence of MFC performance on resistance. The  $I$ - $V$  curve is plotted at different external resistances (10–9999 Ω), as shown in Fig. 2. From this figure we can see that the open-circuit voltage is 639.3 mV. The actual voltage output of the MFC is smaller than the thermodynamically predicted one. Furthermore, the larger the current that is

drawn from the MFC, the lower is the voltage output. The voltage  $V$  decreases almost linearly with the current for small currents. However, after the current increases to a certain value (limiting current as it is called in the literature), the voltage drops off sharply. This is consistent with the one-dimensional model result for conventional fuel cells [9]:

$$V = E_t - (a_A + b_A \ln I) - (a_C + b_C \ln I) - IR_{ohmic} - c \ln \frac{I_L}{I_L - I} \quad (3.2)$$

where  $\eta_{act} = (\alpha_A + b_A \ln I) + (\alpha_C + b_C \ln I)$ , represents the activation loss from both the anode (A) and the cathode (C) based on natural logarithm form of Tafel equation;  $\eta_{ohmic} = IR_{ohmic}$  is the ohmic loss based on the current  $I$  and the ohmic internal resistance  $R_{ohmic}$ ;  $\eta_{conc} = c \ln [I_L / (I_L - I)]$  is the concentration loss, where  $c$  is a empirical constant and  $I_L$  is the limiting current.

The internal resistance of the digital multimeter is as large as  $10\text{M}\Omega$ , so the open-circuit voltage can be taken approximately as the actual electromotive force of the MFC,  $E_t$ . The expression of the anode activation loss ( $a_A + b_A \ln I$ ) is same with that of the cathode activation loss ( $a_C + b_C \ln I$ ), so we may combine them together and fit the experimental results using the following equation:

$$V = V_{open} - (a + b \ln I) - IR_{ohmic} - c \ln \frac{I_L}{I_L - I} \quad (3.3)$$

The fitted result of our experimental results in the form of Eq. (3.3) is given by Eq. (3.4) and shown in Fig. 2.

$$V = 639.30 - 14.30 - 3.15 \ln I - 15I - 77.12 \ln \frac{6.0}{6.0 - I} \quad (3.4)$$

By dividing the electric current  $I$  on both sides of Eq. (3.1), the external resistance is related to the internal resistance  $R_i$  by:

$$R_o = R_t - R_i \quad (3.5)$$

where  $R_t$  is the total resistance and defined by the following equation:

$$R_t = \frac{E_t}{I} \quad (3.6)$$

and  $R_i$  is defined by Eq. (3.7):

$$R_i = \frac{\eta_{act} + \eta_{ohmic} + \eta_{conc}}{I} = R_{act} + R_{ohmic} + R_{conc} \quad (3.7)$$

where  $R_{act}$  is the internal resistance caused by activation losses (activation loss internal resistance, AIR),  $R_{ohmic}$  is caused by ohmic losses (ohmic loss internal resistance, OIR), and  $R_{conc}$  is caused by concentration losses (concentration loss internal resistance, CIR).

As can be seen from Eq. (3.7), the MFC internal resistance consists of three parts, namely, AIR ( $R_{act}$ ), OIR ( $R_{ohmic}$ ) and CIR ( $R_{conc}$ ). The internal resistance calculated from the experimental measurements was plotted against the current in Fig. 3. As can be seen from this figure, with the increase of the current, the internal resistance decreases sharply at first, then remains almost a constant up to 5 mA. If the current increases further, the internal resistance begins to increase sharply.

### 3.2. Activation loss internal resistance (AIR)

The voltage loss due to energy consumption as heat for initiating the oxidation or reduction reactions is the activation loss. According to Eqs. (3.4), (3.5) and (3.7), the activation loss of the MFC is calculated from:

$$\eta_{act} = 14.30 + 3.15 \ln I \quad (3.8)$$

Dividing both sides of the above equation by current  $I$  gives the expression for calculating the AIR of the MFC:

$$R_{act} = \frac{14.30 + 3.15 \ln I}{I} \quad (3.9)$$

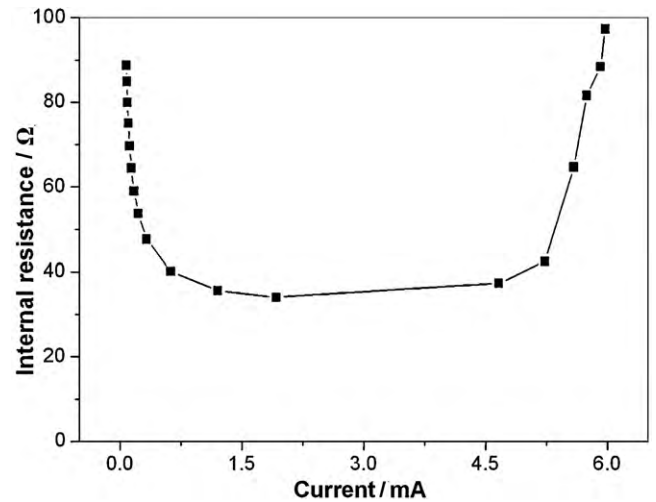


Fig. 3. The internal resistance generated as a function of the current.

Fig. 4 depicts the variation of both the activation loss and the AIR as a function of the current. As can be seen from this figure, the activation loss increases sharply for small current and then after that its increase rate drops and approaches to a constant of about 20 mV. The AIR, on the other hand, decreases very quickly for small current and then the decrease rate is becoming smaller as the current increases and not surprisingly approaches to about  $3\ \Omega$ . In a word, the AIR component of the internal resistance is large at relatively low currents, and becomes smaller with the increase in the current.

### 3.3. Ohmic loss internal resistance (OIR)

The voltage loss due to electric charge transport is called ohmic loss. According to Eqs. (3.4), (3.5) and (3.7), the ohmic loss of the MFC is calculated by the following equation:

$$\eta_{ohmic} = 15I \quad (3.10)$$

From this equation, one can see that the ohmic loss was directly proportional to the current, and the OIR is  $15\ \Omega$  in this experiment. The OIR can take a very large portion of the internal resistance under the moderate current conditions and can be as large as 40%.

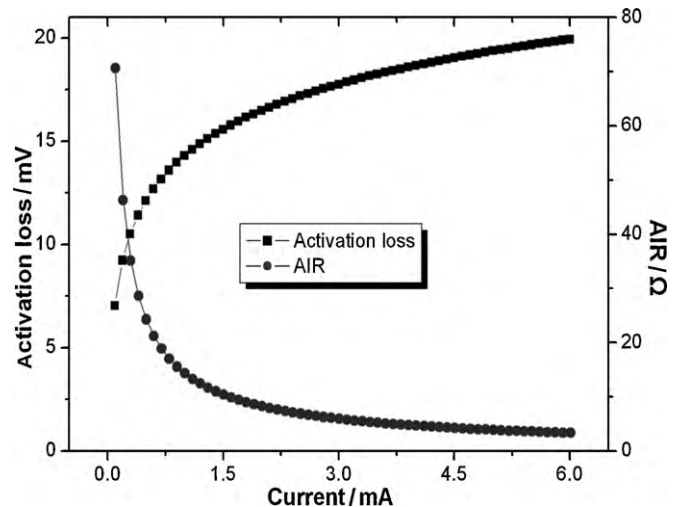


Fig. 4. Variation of the activation loss and AIR with different current.

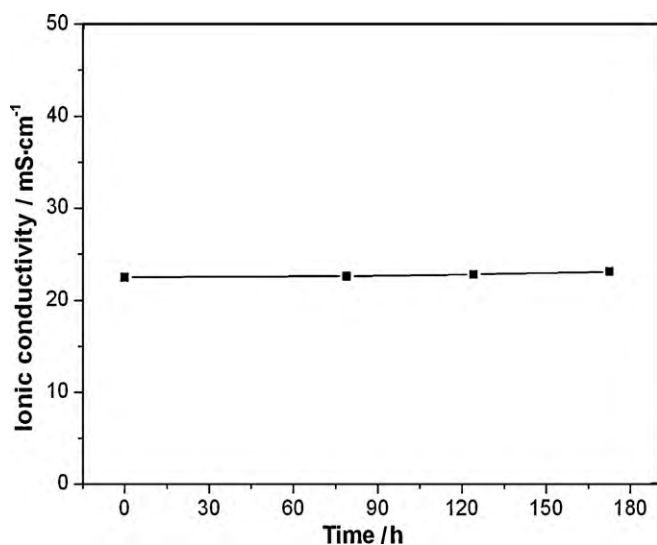


Fig. 5. Variation of the conductivity with time.

The OIR  $R_{\text{ohmic}}$  can also be expressed as according to Wang and Huang [10]:

$$R_{\text{ohmic}} = \frac{L}{A\sigma} \quad (3.11)$$

where  $L$  is the distance, cm;  $A$  is the cross-sectional area,  $\text{m}^2$  over which the ionic conduction occurs;  $\sigma$  is the ionic conductivity of the electrolyte,  $\text{S m}^{-1}$ . The average conductivity of the MFC changed slightly during the whole experimental period. In this experiment it is about  $2.25 \text{ S m}^{-1}$  as shown in Fig. 5. The cross-sectional area was  $2.5 \times 10^{-3} \text{ m}^2$  and the distance was 0.07 m. Therefore, the OIR is  $12.44 \Omega$  according to Eq. (3.11). This result is in good agreement with our experimental measurement ( $15 \Omega$ ) as shown in Eq. (3.10).

#### 3.4. Concentration loss internal resistance (CIR)

The voltage loss due to mass transport is called concentration loss. By using Eqs. (3.4), (3.5) and (3.7), the concentration loss of the MFC is obtained and is calculated by:

$$\eta_{\text{conc}} = 77.12 \ln \frac{6.0}{6.0 - I} \quad (3.12)$$

Dividing both sides of Eq. (3.11) by the current  $I$ , the CIR is obtained for the experimental MFC:

$$R_{\text{conc}} = \frac{77.12}{I} \ln \frac{6.0}{6.0 - I} \quad (3.13)$$

Fig. 6 presents both the concentration loss and the CIR as a function of the current. As can be seen from this figure, the concentration loss increases with the current gradually. However, it turns to increase sharply as the current is approaching to the limiting current (6.0 mA). The reasons for this phenomenon are many. However, the most direct and important one is that as the current increases to its limiting value, the reactions on both of the electrodes approach to their limits and the deposition of micro-organism covers the electrode surface. This may well hinder the mass transfer processes among solution, the PEM, the electrodes and the chambers. This indicates that it is very important to enhance the mass transfer process between the substrate and the electron acceptor to improve the MFC performance.

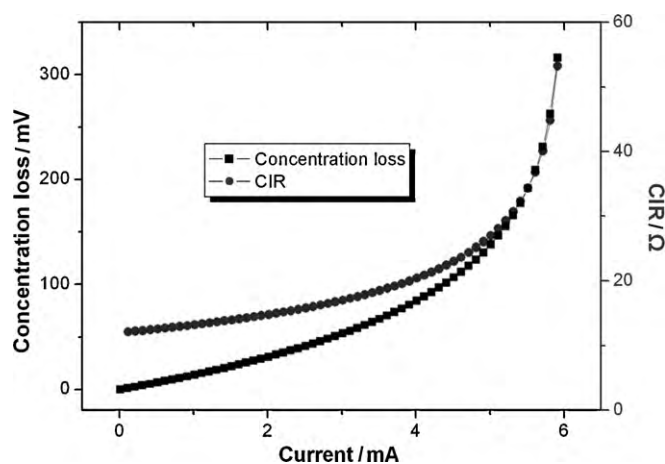


Fig. 6. Variation of the concentration loss and CIR with different current.

#### 3.5. Power output

The internal resistance of a MFC corresponding to the biggest power output is used as a key parameter for evaluating the MFC performance in most literatures. The MFC power output changes with the electric current. To show this, Fig. 7 depicts the variation of the voltage and the power output of the MFC with the electric current for various external resistances (10–9999  $\Omega$ ). As one can see from the  $I$ - $P$  curve shown in Fig. 7, there does exist a special current value (5.0 mA approximately) at which the power output acquire its maximum value (about 2.2 mW). Fig. 8 presents the relation between the MFC power output and the internal resistance. As one can see from this figure, the internal resistance of the MFC corresponding to its maximum power output is about  $42.2 \Omega$ . Furthermore, as indicated by Fig. 9, the maximum power output corresponds to the large concentration loss. This means, to further improve the performance or increase the power output of the MFC, it is of vital importance to reduce its concentration loss.

## 4. Discussion

Fig. 10 shows the variation of the internal resistance  $R_i$  and its components AIR, OIR and CIR of the MFC with current  $I$ . As can be seen from this figure, the internal resistance is almost a constant for  $1 \text{ mA} < I < 5 \text{ mA}$ . The OIR is constant over the whole current region tested, and the variation of the internal resistance with current is resulted from AIR and CIR. To specify the contributions of these

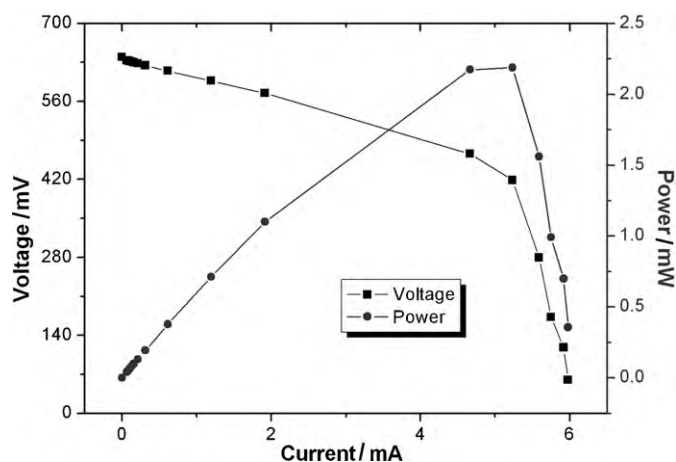


Fig. 7. The power curve after start-up.

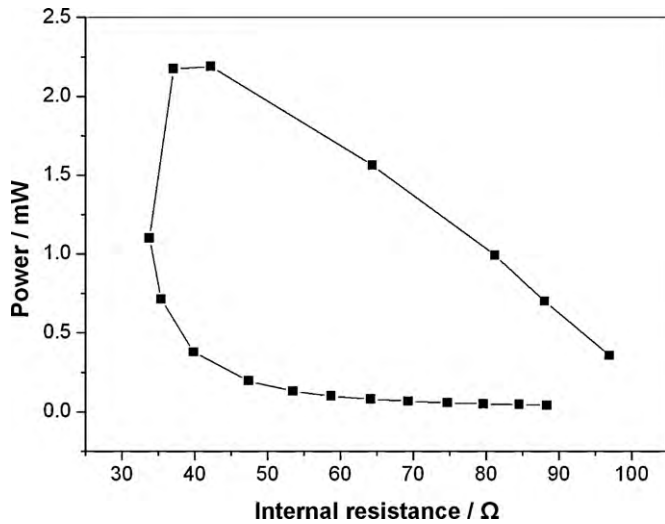


Fig. 8. Power output as a function of the internal resistance.

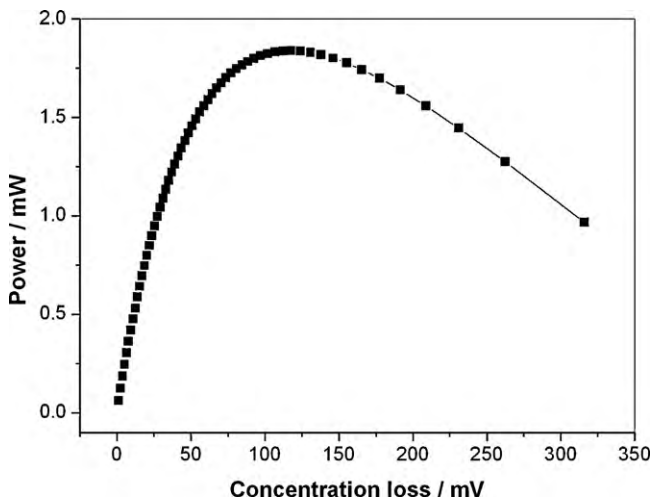


Fig. 9. Power output as a function of the concentration loss.

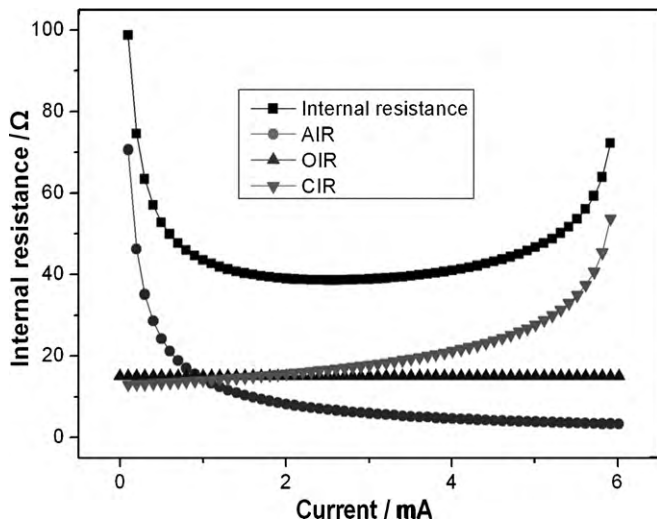


Fig. 10. Variation of the internal resistance with different current.

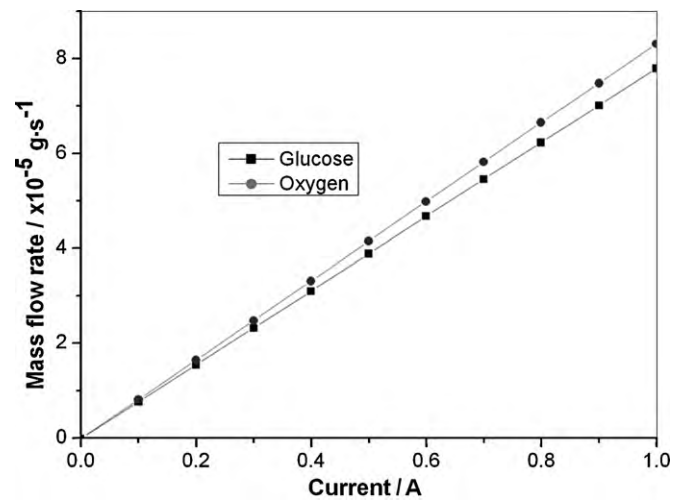


Fig. 11. Mass flow rates of the substrate and electron acceptor with different current.

three components of the internal resistance, we may take the data at 3 mA. The internal resistance is  $38.74 \Omega$  for this specific current, and its component internal resistances are: AIR  $5.92 \Omega$ , OIR  $15 \Omega$  and CIR  $17.82 \Omega$ . The largest of the three components is CIR, which takes up 46% of the total internal resistance. So reducing the concentration loss is the most effective way for improving the MFC performance. Limiting current is the highest achievable current of a MFC, which is 6.0 mA in this experiment. The limiting current is decided mainly by the mass transfer processes of the substrate and the electron acceptor. The mass flow rates of the substrate and the electron acceptor of the MFC of different electric currents using glucose as the substrate and oxygen as the electron acceptor are shown in Fig. 11. From this figure it can be seen clearly, both the mass flow rates increase with current. Increasing the mass flow rates of the substrate and the electron acceptor is an effective way to improve the MFC performance.

The above discussion is made for the given open-circuit voltage or electromotive force. However, according to electrochemistry and thermodynamic theory, increasing the open-circuit voltage will move the  $I-V$  curve to the larger voltage direction, and thus improve the MFC performance. The ideal thermodynamically predicted voltage under the standard condition is as high as 1200 mV [11]. The open-circuit voltage in this experiment is only 639.3 mV, so the performance of the MFC may be greatly improved, at least theoretically.

### 5. Conclusions

The internal resistance of a MFC consists of three parts: AIR, OIR and CIR. The internal resistance is almost a constant for the current is within the region of 1 mA and 5 mA. The largest component of the internal resistance is CIR, which takes nearly 50% of the total internal resistance. The AIR decreases quickly for small current and reduces its decreasing rate as the current increases and approaches to a constant. The OIR is constant over the whole current range and is  $15 \Omega$  for our experimental MFC. Furthermore, the CIR increases slowly with current for small currents. However, as the current approaches to its limiting value, the CIR increases sharply with current. Therefore, increasing the limiting current is an effective way to reduce CIR component and improve the MFC performance. Our work also disclosed that the MFC maximum power output is achieved with large concentration loss. Therefore, it is very important to reduce the concentration loss for improving the performance or increasing the power output of the MFC.

**References**

- [1] B.E. Logan, *Microbial Fuel Cells*, 1st ed., Wiley, New York, 2007.
- [2] X. Cao, P. Liang, *Acta Sci. Circumstantiae*. 26 (8) (2006) 1252–1257.
- [3] P. Liang, M. Fan, *Environ. Sci.* 29 (8) (2008) 2356–2360.
- [4] B. Min, I. Angelidaki, *J. Power sources* 180 (2008) 641–647.
- [5] Q. Wen, Z. Liu, *Acta Phys. Chim. Sin.* 24 (6) (2008) 1063–1067.
- [6] Z. He, *Microbial Fuel Cells: Their Application and Biotechnology*, Washington University, D. Washington, DC, 2007.
- [7] A.K. Manohar, F. Mansfeld, *Electrochim. Acta* 54 (2009) 1664–1670.
- [8] H. Gu, *Studies on Electricity Generation and Wastewater Treatment Abilities of Microbial Fuel Cells*, Zhejiang University, D. Zhejiang, 2007.
- [9] R. O'Hayre, S. Cha, *Fuel Cell Fundamentals*, 1st ed., Wiley, New York, 2006.
- [10] X. Wang, H. Huang, [T] *Fuel Cell Fundamentals*, 1st ed., Publishing House Of Electronic Industry, Beijing, 2007.
- [11] H. Rismani-Yazdi, S. Carver, *J. Power Sources* 180 (2008) 683–694.